Twenty-Seventh Symposium (International) on Combustion/The Combustion Institute, 1998/pp. 453–460

HCO CONCENTRATION IN FLAMES VIA QUANTITATIVE LASER-INDUCED FLUORESCENCE

ERIC W.-G. DIAU,* GREGORY P. SMITH, JAY B. JEFFRIES AND DAVID R. CROSLEY
Molecular Physics Laboratory
SRI International
333 Ravenswood Avenue
Menlo Park, CA 94025-3493, USA

Quantitative laser-induced fluorescence (LIF) measurements of the concentration of HCO are made in three 25-torr methane-oxygen-nitrogen flames: fuel lean ($\Phi = 0.81$), near stoichiometric ($\Phi = 1.07$), and fuel rich ($\Phi = 1.28$). LIF is excited in the (000)-(000) band of the B-X system near 258 nm. The LIF signal from the flame is calibrated against nonflame measurements of a known HCO concentration produced by laser photolysis of acetaldehyde. The LIF signal is adjusted for the variation in the fraction of the population of the laser-excited level as the measured temperature changes with position in the flame and for the measured variation in quenching. The resulting concentration measurements agree well with model predictions for the fuel-lean and near-stoichiometric flame. The measurements in the fuel-rich flame are significantly larger than the model predictions; however, these measurements are subject to increased uncertainty due to the large, broadband background in the rich flame.

Introduction

The formyl radical, HCO, is an important intermediate in methane combustion, and its reactions are important to the determination of flame speed [1–4]. The main reaction sequence in methane oxidation follows the path $CH_4 \rightarrow CH_3 \rightarrow CH_2O \rightarrow HCO$. The important HCO production pathways are the chain propagating reactions of H and OH with formaldehyde. Once formed in a methane flame, several reactions compete to consume HCO. Reactions of HCO with O_2 form HO_2, which inhibits ignition and slows the flame. Reactions with H, CH_3, and OH are chain terminating, reducing the radical pool and the flame speed. These reactions compete with HCO thermal decomposition that forms an atomic hydrogen and increases the flame speed. The HCO mole fraction has recently been found [5] to empirically correlate with the total heat release in a premixed methane-air flame. Thus, HCO is an important combustion intermediate in the chemical mechanism for methane combustion, and its quantitative measurement is an important test for our ability to predict combustion behavior.

We previously made the First observation [6] of the spatial structure of HCO in low-pressure flames, using laser-induced fluorescence (LIF) of the (002)-(000) band of the B-X system near 244 nm; however, that work did not determine an absolute concentration. Absolute HCO measurements using the A-X system have recently been demonstrated by intracavity laser absorption [7] and cavity ring-down spectroscopy [8,9]. In this paper, we make quantitative laser-induced fluorescence measurements of HCO in three 25-torr methane-oxygen-nitrogen flames: near stoichiometric ($\Phi = 1.07$, termed the standard flame), fuel lean ($\Phi = 0.81$), and fuel rich ($\Phi = 1.28$). These measurements are compared to model predictions using detailed chemistry from the GRI-Mech 2.11 [10] chemical mechanism for methane combustion.

Premixed, laminar, low-pressure flames provide an ideal environment for spatially resolved laser-based measurements of flame structure to test chemical mechanisms of combustion [11–13]. The reaction zone in the low-pressure flame is expanded compared to atmospheric pressure, and collimated laser beams can make spatially resolved measurements of the appearance and removal of reactive intermediate species. The reaction time is directly related to the height above the burner.

LIF is well suited for measurements of reactive intermediate species in low-pressure, premixed, laminar flames. The spatial resolution for LIF measurements is determined by the intersection of the probe laser beam with the optical collection solid angle; thus, the burner center line can be well resolved, and profiles of signal versus height above the burner can be measured. Quantitative LIF requires us to relate the signal to the total ground-state number density of the target species, here, the HCO radical. Therefore, we must know the fraction of the total ground-state population excited by the laser,

*Present address: Department of Chemistry, California Institute of Technology, Pasadena, CA 91125, USA

TABLE 1
Flame gas flow rate (slm)

	CH_4	O_2	N_2	Φ
Lean	0.54	1.32	2.91	0.81
Standard	0.66	1.25	2.87	1.07
Rich	0.84	1.31	2.62	1.28

the probability for an excited molecule to emit fluorescence, and the efficiency of optical detection. The specific quantum state excited by the laser is determined from assignment of the LIF excitation spectrum. The fractional population in the absorbing level is then computed from spatially resolved measurements of the gas temperature. The probability to fluoresce is determined from time-resolved LIF measurements of collisional quenching. The efficiency of the optical collection system is determined by calibration using an LIF signal from a known sample of HCO produced by photolysis of acetaldehyde under nonflame conditions.

Experiment

Premixed flames are supported on a 6-cm-diameter porous plug McKenna burner in a low-pressure chamber. Fuel-air stoichiometry is determined by gas-flow measurements, and Table 1 gives the values for the flames studied here. The nitrogen/oxygen ratio in these flames is reduced to stabilize flat flames at low enough pressure to directly measure the time-resolved HCO LIF. The beam from a Nd:YAG-pumped dye (Coumarin 500 for HCO and Rhodamine 640 for OH) laser is directed parallel with the burner surface across the center line of the burner. The fluorescence is collected with *f*/6 optics and spectrally filtered with a bandpass between 340 and 380 nm (combination of WG-345 and UG-11 Schott glass filters). The fluorescence signal is detected by a photomultiplier and either time integrated in a boxcar averager or time resolved with a digital scope.

LIF Signal and Background

HCO is observed by exciting the (000)-(000) band of the B-X system near 258 nm; Fig. 1 shows a portion of the excitation spectrum of HCO from a lean ($\Phi = 0.81$) flame, with the transitions identified from Adamson et al. [14]. We excite a blend of the ${}^qR_0(8)$, ${}^rP_0(4)$, and ${}^rQ_0(7)$ transitions at 258.43 nm to measure flame profiles of HCO. The spectrum has a nonzero baseline of LIF from unidentified hot band and $\Delta K \neq 0$ transitions that underlie the assigned spectrum. For the work here, we assume a baseline value to be that measured at the valley in the spectrum just blue of this blended peak marked with an arrow in the figure. The signal in the ${}^qR_0(8)$, ${}^rP_0(4)$, and ${}^rQ_0(7)$ feature in Fig. 1 is twice that of the background. The LIF from both the peak and the baseline vary linearly with laser pulse energy for values below 100 μJ/pulse, and the fluorescence lifetime of the background is the same as that for the blended peak within measurement uncertainty.

Because the feature we excite is actually a composite of three spectral lines, we must know individual line strengths in order to estimate relative contributions from each absorbing level. Although HCO is actually an asymmetric rotor, its structure is close to a symmetric top, and the quantum number K (actually K_a) is a useful label. Much of the excitation spectrum has the appearance of a parallel band ($\Delta K = 0$) of a symmetric top, except that R and P branch lines with $K' \geq 1$ are asymmetry doubled. In addition, there exist less intense perpendicular branches

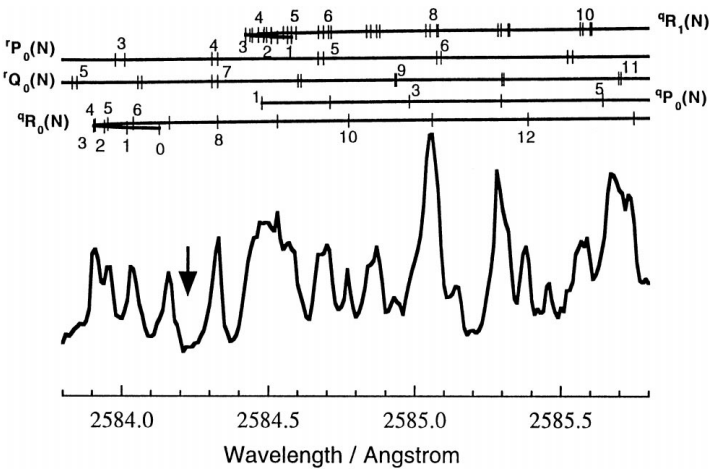

FIG. 1. Laser excitation spectrum near the R band heads of the (000)-(000) band of the HCO B-X system in the lean flame near the peak of the HCO feature. The arrow marks the wavelength used to measure the background LIF.

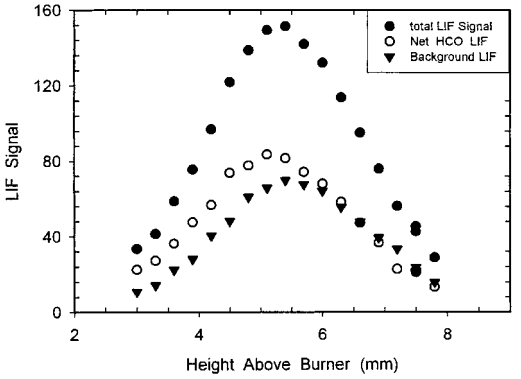

FIG. 2. Total LIF signal (●) and background LIF (▼) measured as a function of height above the burner in the lean flame. The net HCO signal (○) is the difference between the total LIF and the background.

($\Delta K = \pm 1$), showing that the total electronic transition moment lies out of the plane of the molecule [15]. Two of the branches in our blend are perpendicular, and one is parallel. From an analysis of the relative experimental intensities of the two branches, one can estimate [14,16] that the transition dipole lies some 30–40° from the *a* axis. We use this information and Hönl–London factors for a symmetric top [17] to calculate relative line strengths of 1:3:6 for ${}^{r}P_0(4)$, ${}^{r}Q_0(7)$, and ${}^{q}R_0(8)$, respectively. The intensity of the feature is the proportional sum of the temperature-dependent relative populations in each absorbing level weighted by these relative line strengths.

As expected for a reactive intermediate species, we find signal from HCO near the burner surface in the rapid temperature rise of the flame front. Both the total LIF signal and the background vary with height above the burner and flame stoichiometry as shown in Fig. 2. The net HCO LIF from the blended excitation is determined by subtracting the background from the total LIF. The ratio of net HCO LIF to background LIF varies in the lean and the near-stoichiometric flames from 2:1 near the burner surface to 1:1 at the highest locations HCO is observed. Such an increase in background with temperature is consistent with our assumption that the underlying background is an unassigned hot-band LIF from HCO. The background is significantly larger in the rich flame where the net HCO LIF to background ratio varies from 1:1 at a height 2 mm above the burner surface to 1:7 at a height of 8 mm. This much larger background for the rich flame is not consistent simply with our assumption of hot-band HCO LIF, even though the rich-flame temperature is slightly higher.

The measurements in the rich flame are subject to significantly more uncertainty than those in the standard and lean flames. When the LIF background is subtracted from the resonant excitation, we have tacitly assumed that the background is unstructured and originates from other levels of HCO. That is, the background has the same value underneath the HCO transition used for the measurements as in the valley indicated by the arrow in Fig. 1. In the lean and standard flames, this background is at most equal to the net HCO LIF signal, but it is much larger in the rich flame. The uncertainty in the rich-flame measurements is dominated by the constant baseline assumption, which we estimate to be $\pm 10\%$. This is weighted by the background-to-signal ratio in each flame and at the peak of the HCO concentration contributes a $\pm 9\%$ uncertainty in the lean flame, $\pm 10\%$ in the standard, and $\pm 35\%$ in the rich.

We have assumed that the background LIF is produced by hot-band LIF from HCO; however, there are other possible sources of this background. The chemical model predicts several hydrocarbon intermediate species (C_2H_2, HCCO, CH_2OH) in the same region as the HCO that can absorb the excitation light and whose concentrations increase by at least a factor of 2 in the rich flame. For example, C_2H_2 concentrations predicted at the peak of the HCO are 1360 ppm for the rich flame and only 360 ppm in the lean. Acetylene has weakly structured hot-band LIF that can be excited at 258 nm and observed in the detector bandpass. Thus, acetylene could only produce as much as half of the factor of 7 increase in the background seen in the rich flame.

LIF Quantum Yield

The quantum yield, the probability for fluorescence from the excited state, is $\Phi = A/(A + Q + P)$, where A is the Einstein coefficient for radiative emission, Q is the total collisional quenching rate, and P is the predissociation rate. The fluorescence lifetime $\tau = (A + Q + P)^{-1}$ and is measured in these flames by time-resolved fluorescence and ranges between 12 and 20 ns. Because this is significantly shorter than the low-pressure fluorescence lifetime (40–60 ns) [18–20], the dominant removal pathway for laser-excited HCO in these flames is collisional quenching. In each flame, we measure the same fluorescence lifetime for both background and HCO excitation. Figure 3 shows this variation of the collisionally shortened fluorescence lifetime for each of the three flames following 258.43-nm excitation. In the fuel-lean flame (triangles in Fig. 3), we find a nearly constant fluorescence quantum yield versus height above the burner. The lines (linear fit to the data) in Fig. 3 are used to correct the HCO LIF signal for quantum yield variation with height above the burner.

In the fuel-rich flame (squares), we find the

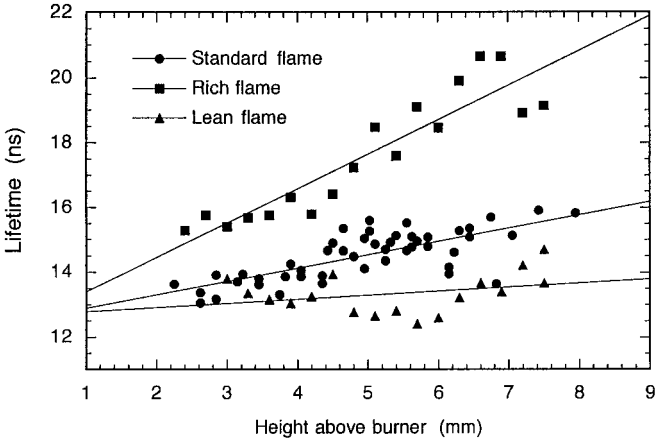

FIG. 3. Fluorescence lifetime of the LIF after exciting a blend of the ${}^{q}R_0(8)$, ${}^{r}P_0(4)$, and ${}^{r}Q_0(7)$ transitions of the (000)-(000) band of the HCO B-X at 258.43 nm in the rich, standard, and lean flames.

quantum yield varies almost twofold across the peak of the HCO LIF signal. The much larger background fluorescence in the rich flame dominates the fluorescence lifetime even at the HCO line excitation, which makes it very difficult to deconvolute the HCO signal fluorescence quantum yield. The observed quantum yield variation with height in the rich flame could be due only to variation from the background. We tried alternate analysis, such as using the lean-flame quenching values, and conclude that the rich-flame [HCO] uncertainty must be increased to $\pm 50\%$.

The measurements in Fig. 3 are consistent with previous measurements [19] of the collisional quenching of B-state HCO at room temperature. Using the predictions for major species mole fractions as a function of height above the burner from our chemical model (discussed later) and the 300 K quenching data, we can estimate the HCO quenching in the flames. Because the quenching measurements of Ref. [19] were made at room temperature, we must estimate a temperature dependence for the collisional quenching. If we assume the quenching rate coefficient is temperature invariant, we predict a quenching rate 30% smaller than observed, whereas if we assume a constant quenching cross section, we predict a quenching rate 40% larger than observed. The observation of fastest quenching in the lean flame and slowest in the rich flame is predicted by the model. Without knowledge of the temperature dependence of the rate constants for quenching of excited HCO, we cannot draw more specific conclusions.

Gas Temperature

Gas-temperature measurements are necessary to infer quantitative HCO mole fractions from LIF signals. The LIF signal must be corrected for temperature variation of the Boltzmann population fraction in the ground state, the overlap between laser and Doppler broadened line shapes, and the change in gas density. We determine gas temperature from LIF measurements of the OH rotational distribution as a function of height above the burner; the increased quantum yield and axial diffusion in the low-pressure flame allows OH temperature measurements at low temperatures just above the burner surface. We have previously demonstrated such measurements can produce an accurate temperature profile [1,21,22]. The temperature profiles for the fuel-lean, near-stoichiometric (standard), and fuel-rich flames are plotted as solid lines in Figs. 4–6.

Quantitative HCO Measurements

The HCO LIF detection efficiency is calibrated by comparison to LIF from the known amount of HCO produced by 308-nm photolysis of acetaldehyde flowing through the burner chamber at 0.32 torr. We select the uniform center of the 308-nm light beam from an excimer laser and measure the absorption; from Horowitz et al. [23], we assume that 93% of the absorbed photons yield an HCO molecule, thus providing a known HCO concentration n_c. In addition to producing HCO, photolysis can heat the gas. By limiting the photolysis energy to a few mJ over an 8-mm diameter, the gas temperature rise is less than 50 K. Photolysis also can produce a nonthermal state distribution in the product HCO. The probe laser is delayed 20 μs to allow for collisional cooling of the product HCO; the LIF signal is constant to $\pm 5\%$ for delays of 10–30 μs. The background LIF is only a few percent of the calibration signal. We confirm that the HCO LIF is linear in both the photolysis and the probe LIF laser pulse energies. The resulting LIF excitation spectrum from the calibration HCO compares well with earlier 300 K flow-cell measurements in our laboratory [15].

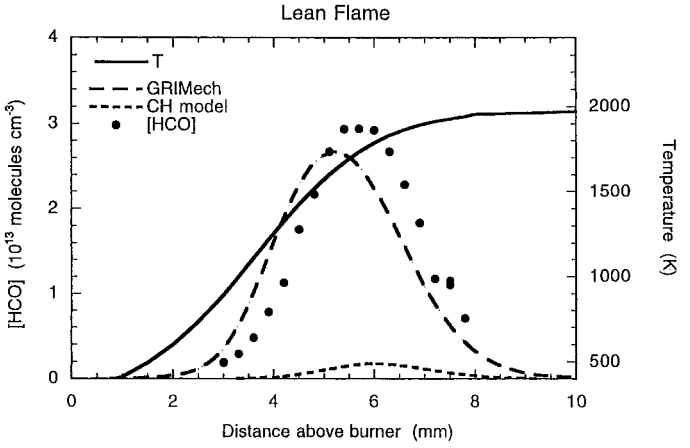

FIG. 4. HCO concentration measured by LIF (●) and predicted by model (dashes) versus height above the burner for the lean (Φ = 0.81) flame. The solid line is the measured temperature profile, and the short dashed lines show the position of the CH structure in this flame.

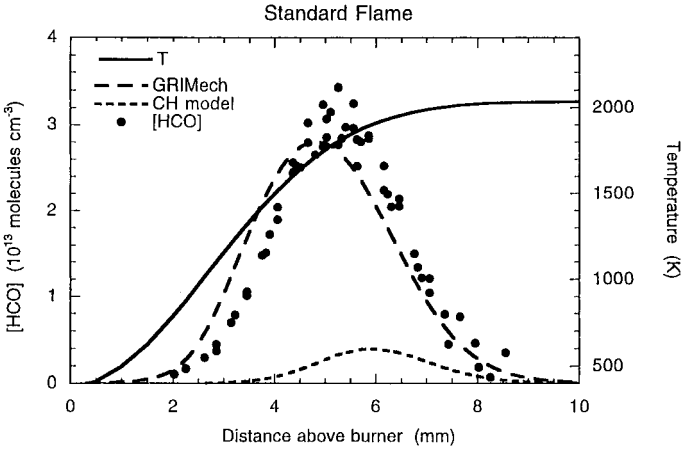

FIG. 5. HCO concentration, gas temperature, and CH concentration versus height above the burner in the near-stoichiometric (Φ = 1.07) flame (as in Fig. 4).

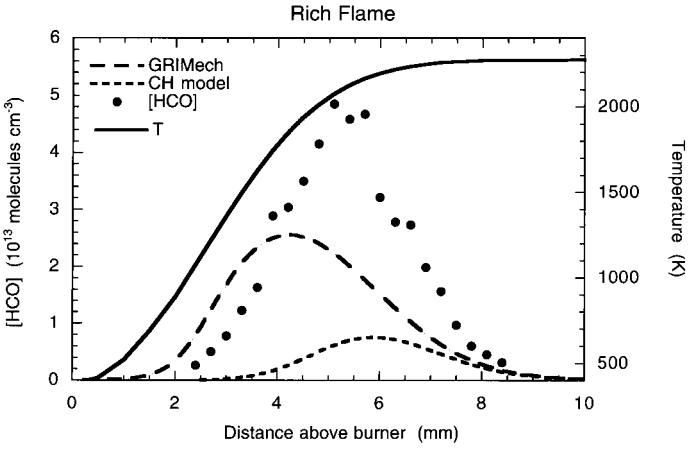

FIG. 6. HCO concentration, gas temperature, and CH concentration versus height above the burner in the rich (Φ = 1.28) flame (as in Fig. 4).

The HCO concentration in the flame, n_F, is determined from the ratio of the HCO LIF in the flame, S_F, and calibration, S_c:

$$n_F = n_c \times S_F/S_c \times f_B(T_c)/f_B(T_F)$$

$$\times \tau_c/\tau_F \times E_c/E_F \times \Gamma_c/\Gamma_F$$

where the Boltzmann fraction, $f_B = N_J/(Q_{\text{rot}} \times Q_{\text{vib}})$, with N_J the population in the Jth rotational level and Q_{rot} and Q_{vib} the respective partition functions. The Boltzmann fraction for the blended transition excited is the sum for the three lines weighted by their relative line strengths. The ratio is calculated for the flame temperature T_F and the calibration T_C. τ_c/τ_F is the ratio of fluorescence lifetimes, E_c/E_F, is the ratio of excitation laser pulse energies, and Γ_c/Γ_F is the ratio of overlap integral between the excited transitions and the laser bandwidth. For our 0.5-cm^{-1} laser bandwidth, the overlap integrals are nearly equal for both the calibration and flame temperature. The ratio does not depend on the Einstein A coefficient for the excited levels; although fluorescence lifetimes have been measured at low pressures [24], and the radiative lifetime has been calculated [20], the degree of HCO B-state predissociation is not well known.

There is a very large temperature variation in the ratio of the Boltzmann fractions arising from the difference in the rotational and vibrational partition functions at the calibration and flame temperature. Over the temperature range between the low ~900 K near the burner where HCO First begins to appear and the ~2000 K where HCO has been consumed, the ratio of the Boltzmann factor varies by nearly a factor of 7.

In addition to the background, there are other sources of uncertainty in the HCO measurements. The fluorescence lifetime is measured to ±1 ns that produces a 5% error in the relative quantum yield. The partition function of HCO varies by ±10% over the ±60 K uncertainty in the gas-temperature measurement. For the calibration experiment, we measure the acetaldehyde absorption cross section for the 308-nm laser pulse to be $3.18 \pm 0.25 \times 10^{-20}$ cm^{-2}. The photolysis laser pulse energy is known to ±5%, and the HCO photolysis yield is known to ±3%. These uncertainties combine with the 5% statistical errors for both calibration and flame LIF to produce an additional 11% uncertainty for the calibration procedure. Propagating these values with that associated with the background subtraction yields a total uncertainty of ±18%, ±20%, and ±50%, in the lean, standard, and rich flames, respectively.

The HCO LIF signals from both the blended transition and the baseline are measured versus height above the burner for fuel-lean, near-stoichiometric (standard), and fuel-rich flames. The difference between these signals at each height in the flame is corrected for the temperature variation of the Boltzmann fraction of HCO in the excited transition blend and for spatial variation of the fluorescence quantum yield. The corrected LIF measurements are then converted to HCO concentrations from the calibration. The HCO LIF concentration measurements versus height above the burner are plotted as points in Figs. 4–6 for the fuel-lean, near-stoichiometric (standard), and fuel-rich flames. The HCO rises faster than the temperature and reaches its peak concentration before either the OH radical or the temperature reaches 75% of its peak value. The peak HCO concentration in both the fuel-lean and standard flames are nearly identical, with 50% more HCO in the fuel-rich flame. The peak HCO concentrations in our lean ($\Phi = 0.81$), standard ($\Phi = 1.07$), and rich ($\Phi = 1.28$) 25-torr flames are $2.8 \pm 0.5 \times 10^{13}$ cm^{-3}, $3.0 \pm 0.6 \times 10^{13}$ cm^{-3}, and $4.8 \pm 2.4 \times 10^{13}$ cm^{-3}, respectively. If the rich flame data were analyzed with the invariant lean flame fluorescent lifetime, fuel-rich flame measurements would be 15% larger at the peak and 50% larger at 8 mm above the burner. These values are in agreement with the cavity ring-down measurement [8] but are slightly larger than the later reports [9].

Flame Chemistry Model

The flame chemistry is modeled with the Sandia PREMIX code and CHEMKIN package [25] using the GRI-Mech™ 2.11 chemical mechanism [10] for methane combustion. The one-dimensional transport in PREMIX is suitable on the center line of our stable, laminar, premixed flame. The combustion mechanism includes 49 species and 279 pressure- and temperature-dependent reactions (plus their reverse). The measured temperature profile and gas-flow rate (Table 1) are used to constrain the calculation. The prediction for HCO is plotted in Figs. 4–6; the predicted CH is also indicated to relate the HCO structure to the position of the CH in the flame front. Quantitative LIF measurements of CH in similar flames are in excellent agreement with these predictions [11,26,27]. We find the predicted HCO profile to be slightly wider and closer to the burner than the measurements in all three flames. Like the measurements, the model predicts nearly the same HCO peak concentration in the lean and standard flames, with an increase of peak HCO in the rich flame. Quantitative agreement is found for the lean and standard flames, and the model underpredicts the less certain HCO concentration in the rich flame.

Sensitivity analysis relates the predicted HCO concentration to changes in the reaction rate constants: $S_i \equiv \partial(\ln[\text{HCO}])/\partial(\ln k_i)$; where S_i is the sensitivity coefficient and k the rate constant for the ith reaction. A sensitivity coefficient of -1 means that

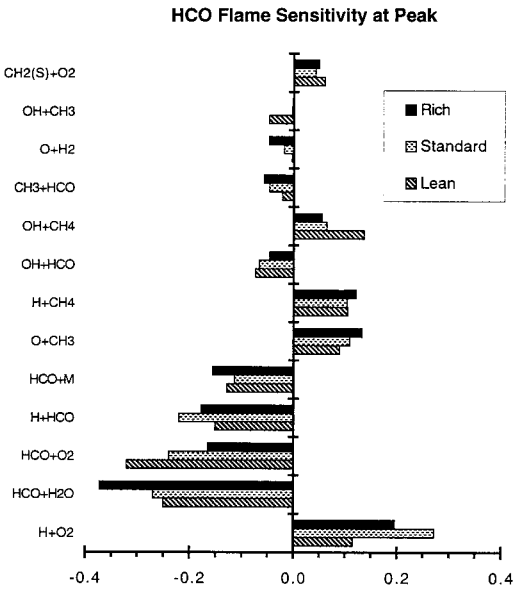

FIG. 7. Sensitivity coefficients (see text) for the HCO concentration at its peak for the fuel-lean, near-stoichiometric, and rich flames.

the concentration is reduced by a factor of 2 if k is doubled. Thus, large absolute values of S_i indicate which reactions are important to the HCO concentration. Figure 7 shows all of the reactions that have peak HCO sensitivity coefficients $|S_i| > 0.05$. Those reactions that might be involved in the disagreement between model prediction and LIF measurement in the rich flame should have similar sensitivities in the lean and standard flame and a much larger sensitivity in the rich flame. Two reactions, thermal decomposition of HCO energized by water collisions and O-atom attack on H_2, are the only reactions that meet this criteria. The temperature and collider dependence of thermal decomposition is poorly understood and could be the major source of the disagreement between model and measurement of HCO concentration.

Conclusions

An isolated, assigned transition has been selected and used to perform quantitative HCO concentration measurements in three low-pressure methane and synthetic-air flames. LIF in the B-X (000)-(000) is calibrated by acetaldehyde photolysis. Good agreement between the measured HCO concentration and model calculation is found for a fuel-lean and near-stoichiometric flame. In a rich flame, the large measured increase in peak HCO concentration is not predicted by the model; however, the rich-flame measurements are subject to significant uncertainty. A background LIF signal underlies the HCO LIF in all three flames, and this background is more than five times larger in the rich flame. The potential errors associated with the background subtraction limit the accuracy of the HCO concentration measurements. Future applications, especially LIF imaging in rich environments, will require additional diagnostic development to identify and quantify the background interference. The partition function of polyatomic molecules has a very large variation with temperature, and even relatively precise (± 60 K) temperature measurements produce significant uncertainty ($\pm 10\%$) in the HCO concentration.

Acknowledgments

We acknowledge support for this work from the Basic Research Group of the Gas Research Institute. We thank Jorge Luque for numerous discussions on the subtleties of quantitative laser-induced fluorescence.

REFERENCES

1. Westbrook, C. K. and Dryer, F. L., *Prog. Energy Combust. Sci.* 10:1 (1984).
2. Warnatz, J., in *Combustion Chemistry,* Springer-Verlag, Berlin, 1984, p. 197.
3. Olsson, J. O. and Andersson, L. L., *Combust. Flame* 67:99 (1987).
4. Kee, R. J., Miller, J. A., Evans, G. H., and Dixon-Lewis, G., in *Twenty-Second Symposium (International) on Combustion,* The Combustion Institute, Pittsburgh, 1989, p. 1479.
5. Najm, H. N., Paul, P. H., Mueller, C. J., and Wyckoff, P. S., *Combust. Flame,* 113:312 (1998).
6. Jeffries, J. B., Crosley, D. R., Wysong, I. J., and Smith, G. P., in *Twenty-Third Symposium (International) on Combustion,* The Combustion Institute, Pittsburgh, 1990, pp. 1847–1854.
7. Cheskis, S., *J. Chem. Phys.* 102:1851 (1995).
8. Scherer, J. J. and Rakestraw, D. J., *Chem. Phys. Lett.* 265:169 (1997).
9. Scherer, J. J., Aniolek, K., and Rakestraw, D. J., "Cavity Ringdown Laser Absorption Spectroscopy of Polyatomic Radicals in Low-Pressure Flames," *American Chemical Society Symposium Series,* Washington, D.C., 1998, in press.
10. Bowman, C. T., Hanson, R. K., Gardiner Jr., W. C., Lissianski, V., Frenklach, M., Goldenberg, M., and Smith, G. P., "GRI-Mech—An Optimized Detailed Chemical Reaction Mechanism for Methane Combustion and NO Formation and Reburning," Gas Research Institute report no. 97-0020. Refer to the GRI-Mech homepage at http://www.me.berkeley.edu/gri_mech/.
11. Berg, P. A., Hill, D. A., Noble, A. R., Smith, G. P., Jeffries, J. B., and Crosley, D. R., "Absolute CH

Concentration Measurements in Low-Pressure Hydrocarbon Flames: Comparisons with Model Results," AIAA 97-0905.
12. Harrington, J. E., Smith, G. P., Berg, P. A., Noble, A. R., Jeffries, J. B., and Crosley, D. R., in *Twenty-Sixth Symposium (International) on Combustion,* The Combustion Institute, Pittsburgh, 1996, pp. 2133–2138.
13. Heard, D. E., Jeffries, J. B., Smith, G. P., and Crosley, D. R., "LIF Measurements in Methane/Air Flames of Radicals Important in Prompt-NO Formation," *Combust. Flame* 88:137 (1992).
14. Adamson, G. W., Zhao, X., and Field, R. W., *J. Molec. Spectrosc.* 160:11 (1993).
15. Sappey, A. D. and Crosley, D. R., *J. Chem. Phys.* 93:7601 (1990).
16. Lee, S.-H., Chen, I.-C., Adamson, G. W., and Field, R. W., *J. Molec. Spectrosc.* 182:385 (1997).
17. Zare, R. N., in *Angular Momentum,* Wiley, New York, 1988, p. 286.
18. Lee, S.-H. and Chen, I.-C., *J. Chem. Phys.* 105:2583 (1996).
19. Meier, U. E., Hunziker, L. E., and Crosley, D. R., *J. Phys. Chem.* 95:5163 (1991).
20. Manaa, M. R. and Yarkony, D. R., *J. Chem. Phys.* 100:473 (1994).
21. Rensberger, K. J., Jeffries, J. B., Copeland, R. A., Kohse-Höinghaus, K., Wise, M. L., and Crosley, D. R., *Appl. Opt.* 28:3556 (1989).
22. Crosley, D. R. and Jeffries, J. B., "Temperature Measurements by Laser-Induced Fluorescence of the Hydroxyl Radical," in *Temperature: Its Measurement and Control in Science and Industry,* vol. 6, American Institute of Physics, New York, 1992, p. 701.
23. Horowitz, A., Kershner, C. J., and Calvert, J. G., *J. Phys. Chem.* 86:3094 (1982).
24. Tobason, J. D. and Rohlfung, E. A., *Chem. Phys. Lett.* 252:333 (1996).
25. Kee, R. J., Grcar, J. F., Smooke, M. D., and Miller, J., "A FORTRAN Program for Modeling Steady Laminar One-Dimensional Flames," Sandia National Laboratories report no. SAND85-8240.
26. Luque, J. and Crosley, D. R., *Appl. Phys. B* 63:91 (1996).
27. Luque, J., Smith, G. P., and Crosley, D. R., in *Twenty-Sixth Symposium (International) on Combustion,* The Combustion Institute, Pittsburgh, 1996, p. 959.

COMMENTS

Katherina Kohse-Höinghaus, Universität Bielefeld, Germany You have demonstrated the potential of HCO measurements in capturing heat release. Because many groups may want to use this in different flame situations, would you have any particular recommendations for quantitative 2-D measurements of HCO?

Author's Reply. The results shown here demonstrate the potential for large variation as a function of fuel–air stoichiometry of the background signal that underlies the HCO LIF. Therefore, it is necessary to carefully measure this background in any quantitative heat-release determination. This would limit the LIF strategy presented here to steady flames where separate measurements of the background and the signal plus background are possible.

•

Volker Sick, The University of Michigan, USA. Did you spectrally resolve the LIF emission to further investigate the origin of the background signal?

Author's Reply. No. Further work to optimize the HCO signal to background is certainly needed.

•

Terrill A. Cool, Cornell University, USA. With regard to the source of the background signal, it may be reasonable to assign the source to HCO. In our previous measurements of HCO in methane/oxygen flames, using the REMPI method, we have also observed a strong quasi-continuum background. This background signal varies with flame stoichiometry and with distance from the burner in the same way as did the resonant HCO signal. Second, because you get a CH_3 radical for each CHO when you dissociate acetaldehyde, have you plans to use this approach for calibration of measurements of the CH_3?

Author's Reply. The background feature lies a bit higher above the burner than the HCO structure; thus, if the background is due to HCO, it arises from hot bands that have a signal with a different temperature dependence than the signal from (0,0,0)–(0,0,0) B–X. Before speculating further on the origin of the background signal, more work is needed. Your suggestion that we also use this calibration approach for methyl radicals is excellent. We will use it when we return to measurements of that species in our laboratory.

•

S. Cheskis, Tel Aviv University, Israel. Did you try to see the same background structure that you saw in flame in your calibration experiments? If it is from "hot" HCO bands, it could be seen at a short time after photolysis and before the thermalization.

Author's Reply. In the presentation, the HCO LIF signal from photolysis shows only a small background signal. The signal-to-background ratio is a constant 10:1 and does not vary over the range of photolysis energies used. We did not examine the signal to background at short delays after the photolysis laser pulse.